



The Two-Center-Shell-Model for Analyzing the Dynamics of Heavy Ion Collisions

Sabahat Sadiq lone, Priyanka, M.S.Mehta

department of physics, Rayat Bahra University, Mohali-140 104, India.

Abstract:-

Current findings from using the shell model in nuclear fission and heavy-ion collisions are discussed. Since Nilsson-style one-centre oscillators are incapable of producing the scission configuration seen in fission, a new model based on a two-centre shell has been developed to account for it. The discovery of the compound nucleus in fission and its subsequent creation as a byproduct of heavy-ion collisions has led to the formulation of a hypothesis of fragmentation. The well-established Cranking model and the two-centre shell model (in the Stutinsky style) both show this to be the case. Under certain limiting circumstances, the time-dependent Schrodinger equation is solved for the fission and heavy-ion collision trajectories by using the mass and charge asymmetries of the two components as dynamical coordinates in the Hamiltonian. The concept has significantly increased the yields from binary fission and the methods for creating new elements, including super-heavy elements, by the fusion of two heavy ions. In light of the recent discovery of fissioning of a heavy (compound) nucleus produced in heavy-ion collisions, extensions of the shell model to two and more centers have also been conducted. Based on current trends in experimental data, it seems that characterizing nuclear fission and heavy ion collisions properly requires treating the nucleus as a multi-centre shell. In this article, we take a look back at the two-centre shell model and the main theoretical challenges in describing heavy-ion collisions at high energies.

Keywords: Heavy ion collision, fission, two-centre shell model

1. INTRODUCTION

“Prior knowledge was restricted to single-shell models. We display the potentials for the two-shell model. In particular, the Nilsson model has been used to explain nuclear structure-related phenomena in deformed nuclei. Long, stretched cigar-like structures called "needle-ellipsoids" are the only way the Nilsson model may asymptotically approach the equipotential surfaces when the deformations are sufficiently enough (see fig. 1). As can be observed in Fig. 1, as the amount of deformation grows, so does the zero-point energy. Therefore, the energy of a single particle rises as a direct consequence. The surface of the collective potential energy, which is basically the sum of single-particle energies, approaches infinity for very



large deformations and does not lead to a fission barrier. Strutinsky suggests applying the shell modifications from the Nilsson model to an orderly liquid-drop barrier as a way to fix this problem. This phenomenological approach seems to make sense at first glance, but the mechanics of implementing these alterations to the shell remain unclear. As a rule, it's due to human contact. Gravity, electromagnetism, weak nuclear forces, and strong nuclear forces are the four basic forces that describe the interactions between the fundamental building components of matter. Except for gravity, local gauge theories provide a tried-and-true microscopic quantum account of all of these interactions. According to these models, the fundamental constituents of matter are spin-1/2 fermions interacting with one another via the propagation of spin-1 boson exchanges. This system relies heavily on the Higgs spin-0 boson, the single basic scalar particle in the Standard Model, since all other fields gain mass in direct proportion to their connection to the Higgs. Until now, the Higgs boson, which was discovered at the Large Hadron Collider in 2012, has fulfilled all of the Standard Model's predictions. Though general relativity, a classical field theory of gravity, has been empirically proved, a theory of quantum gravity has eluded researchers until very recently. Gravitational waves, which are produced when huge compact objects like black holes or neutron stars collide, are the most recent of these confirmations (and possible experimental probes are far out of reach for the foreseeable future). Nuclear strength QCD, the microscopic theory of strong nuclear interactions, was developed in the early 1970s with the help of numerous experiments. Proton charge is said to be compressed into weaker components with spin 1/2 that interact at high momentum transfer but are unresolved in scattering, as shown by the observed structure functions. This was seen in deep inelastic electron scattering from proton targets. Due to these findings, it is now conceivable to formulate a non-Abelian gauge theory with asymptotic freedom, a theory in which the coupling strength diminishes with distance. This, along with other results from hadron spectroscopy, led to the development of an SU(3) gauge theory, which explains spin-1/2 matter fields (the quarks) at their most basic level. Bound hadronic states need strong interactions between quarks, yet deep inelastic scattering investigations show that quarks interact very weakly. The asymptotic freedom property of QCD, which stipulates that the strong coupling constant grows small at short distances and big on distance scales relative to the size of a proton, resolves this conflict. We now know that the top quark has a mass of roughly 175 GeV [1], whereas the mass of the other quarks ranges from almost massless to down to odd to charm to bottom to top.

Up and down quarks make up the whole of atomic nuclei in regular matter, whereas heavier quarks are only found in heavier hadrons (at the exception of the top quark, whose lifetime is so short that it decays before bound states can be formed). As the best microscopic theory to explain strong nuclear interactions, QCD has been the recipient of a great deal of experimental support [2]. However, for the most quantitative comparisons between theory and experiment, asymptotic freedom necessitates strict techniques (i.e., processes involving at least one hard



momentum particle in the final state). Even while QCD has been shown to accurately portray strong nuclear interactions, it cannot account for the nuanced properties of nuclear matter at extremes of temperature and pressure. Asymptotic liberties, constraints, and reductions are discussed. Due to their inability to exist freely, quarks and gluons must instead create bound states (the hadrons) in which their color charge is "hidden." This is one of the most important features of quantum Chromodynamics (QCD). When a quark is removed from a hadron, more hadrons are produced (for instance, by colliding with another hadron at a high energy). However, the average distance between hadrons falls when several are packed together, leading to weaker interactions¹. Because of this, we may deduce that the forces that confine quarks inside hadrons would ultimately weaken to the point where quarks are no longer restricted in their motion. Quark-gluon plasma is the name given to the particular phase of nuclear matter (QGP) ([3]). Since the coupling constant is still too big at this energy scale for perturbation theory to be used safely, this transition cannot be described as perturbative. However, by discretizing Euclidean space-time on a lattice, it is possible to express QCD in a non-perturbative manner. [4] Because of this setup, just some of the observables need to increase by a power law for their calculation to be possible. The expected value of the trace of a Wilson loop (which may be attributed to the potential between a pair of infinitely heavy quarks and antiquarks) and the entropy density are two measurable parameters in lattice QCD that are associated with the confinement/deconfinement transition (that measures the number of active degrees of freedom in the system). Furthermore, by adjusting these and other lattice QCD theory parameters, we may be able to probe the impact of factors like the number of quark families and their masses on the observed events.

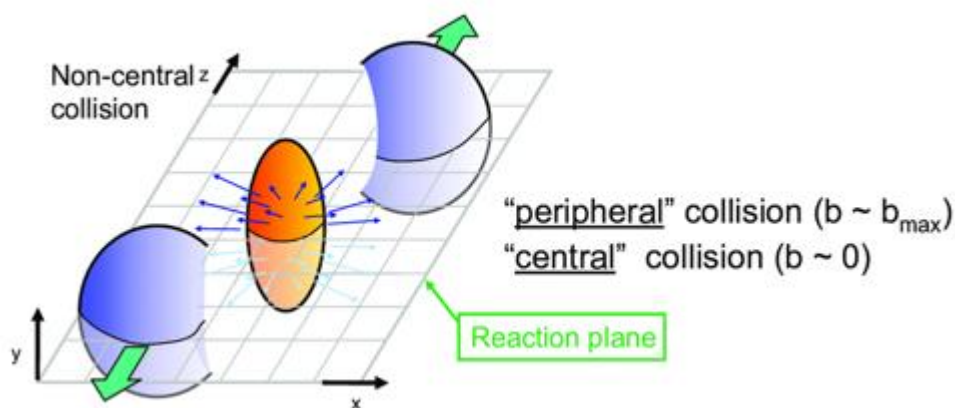


Figure 1 Reaction process

An estimated heavy ion impact geometry. In this instance, x and y are the transverse coordinates, whereas z represents the collision (or longitudinal) axis. The interaction zone—



the region where the two nuclei overlap—is emphasized. The entire number of atoms is shown by the symbol N , which stands for the nucleon count. The response plane crosses the interaction zone horizontally (x, z)”.

2. HISTORY OVER HEAVY ION COLLISIONS

While the confinement transition occurred just a few microseconds after the Big Bang, no physical remnants of this period can be found in our present-day cosmos. In the 1980s, scientists investigated the possibility of creating dense, high-temperature nuclear matter by colliding heavy nuclei. Heavy ion collisions have been the subject of, or a part of, a number of subsequent research. The Lawrence Berkeley National Laboratory in California, USA, built the Bevatron in 1954, and it remained in use there until 1993. Millions of electron volts Synchrotron. Since 1960, scientists from all around the world have been able to use the Alternating Gradient Synchrotron at Brookhaven National Laboratory in New York. (AGS). Current practice involves the RHIC injector. Since its inception in 1976, the Super Proton Synchrotron (SPS) has played a crucial role in CERN's scientific endeavors. An aside: this is the LHC injector. Since 2001, GSI has been home to the Schwer-Ionen-Synchrotron. (SIS-18). Since 2009, researchers from the European Organization for Nuclear Research (CERN) have made use of the Relativistic Heavy Ion Collider (RHIC) at the Brookhaven National Laboratory in New York. The CERN SPS, which collided heavy ions with a center-of-mass energy of 17 GeV, discovered the first experimental evidence of a deconfinement transition. Rather of focusing on whether or whether a quark-gluon plasma is created, higher energy experimental endeavors (such the RHIC at Brookhaven National Laboratory and the Large Hadron Collider at CERN) are now exploring some of its properties statistically [5].

2.1 Experimental handles

“The conditions under which quark gluon plasma may be created in heavy ion collisions are sensitive to a number of experimental controls. One such element is the amount of nucleons colliding, which has a profound effect on the size of the contact zone . Another variable that has an instantaneous effect on the volume when colliding with certain ion species is the impact parameter of each collision. There is a strong relationship between the impact parameter and other variables, even if it is not immediately apparent (such as the total multiplicity in the end state or the transverse energy). Finally, the energy of a collision may change the density of the net baryons produced and hence the initial energy density (temperature) (although of course, this is in reality strongly confined by the accelerator design). This causes heavy ion tests to exhibit many phases at various depths, as seen in Figure 2”.

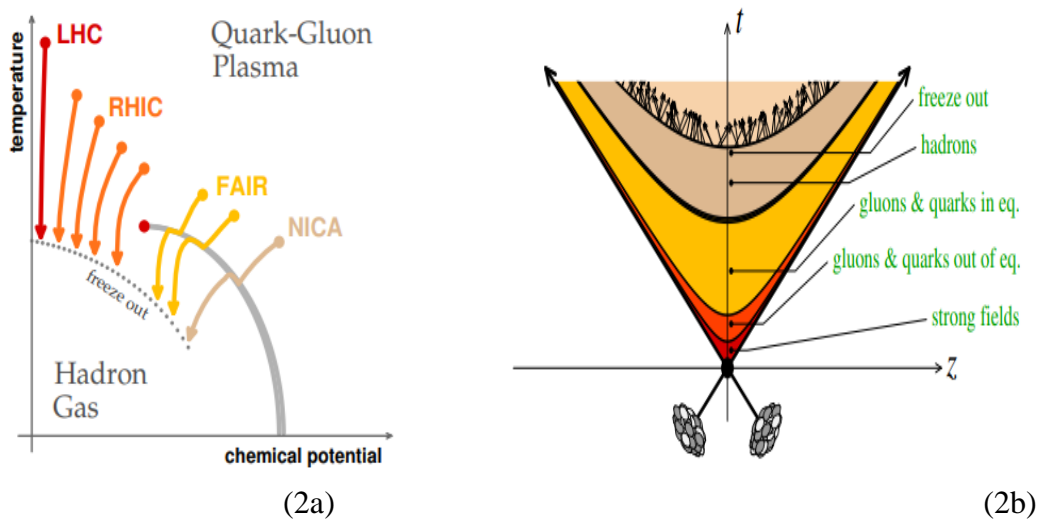


Figure 2 heavy ion collisions

3. STAGES OF HEAVY ION COLLISIONS

A collision between two nuclei moving at ultrarelativistic speeds may potentially be broken down into multiple phases, as seen in Figure 2. Since the boost is rather constant (it doesn't depend on the spatial velocity variable), this representation results in a meaningful ordering of encounters and their aftereffects: $s \propto 1/2 \ln((t+z)/(t-z))$. The actual collision only takes a few instants due to Lorentz contraction of the nuclei in the laboratory frame. Shortly after a collision, gluons that have not yet found equilibrium make up the vast majority of the newly produced matter (they are not even on-shell at the very beginning, and the system is better treated in terms of fields rather than particles). High gluon occupancy number matter is highly interacting and gravitates toward equilibrium (both kinetic and chemical, since quark-antiquark pairs are produced in the process). In hindsight, it is feasible that the system's overall development might have been described using virtually flawless (i.e., with extremely tiny values of the viscous transport coefficients) relativistic hydrodynamics over most of its existence. When a system is expanded, its temperature drops until it reaches the confinement temperature. If the system is kept in a nearly equilibrium condition, the confinement transition will be recorded in the equation of state, making its crossing very obvious from a hydrodynamics perspective. When a system's concentration drops and its mean free path lengthens, kinetic theory excels over hydrodynamics as the best framework for understanding the system's development. It is predicted by this model that the cross-section values determine the order in which inelastic processes (chemical freezeout) and kinetic freezeout (no change in the momenta of the particles) cease to operate (afterwards, all particles therefore fly on straight lines at constant velocity until they hit a detector)



4. MAIN ASPECTS OF HEAVY ION COLLISIONS:

“Normal nuclear matter, above a particular temperature and density, is thought to give rise to deconfined quark-gluon matter. Normal nuclear matter (p, n, pions, Deltas, etc.) exists at low temperatures and densities, and is composed of hadrons, whereas quark-gluon matter (u, d, s, in 3 colors), and unbound gluons, exist as subatomic particles.

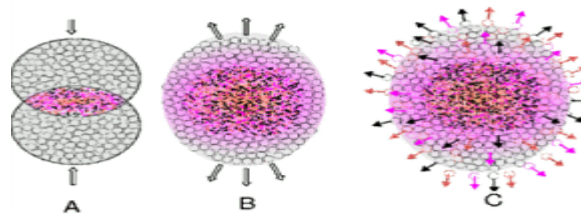


Figure (3a,b,c)

Figure 3 Heavy ion collisions

In the lab, quark-gluon matter might be created by the high-energy collisions of heavy ions, which could provide enough heat and compression.

4.1 Space time diagram for the time evolution of the colliding system

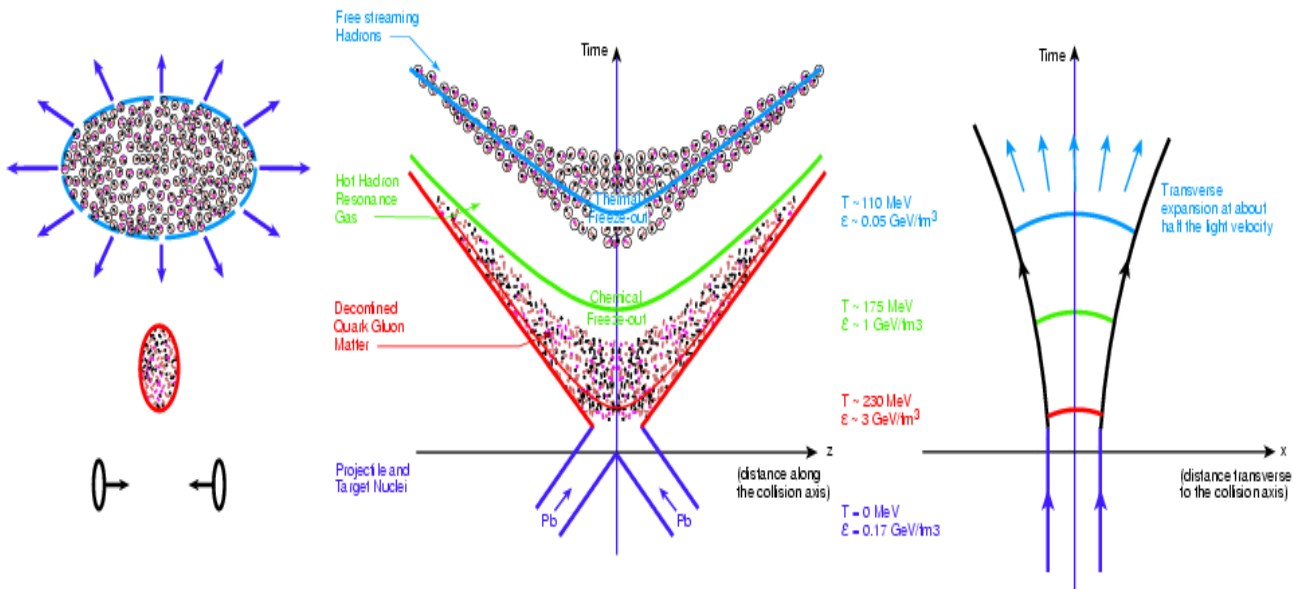


Figure 4 evolution of the colliding system

At $t=0$, the first collision between the two nuclei occurs. After this, at a time of $t \sim 1 \text{ fm}/c \sim 3 \times 10^{-24} \text{ sec}$, a new state of quark-gluon matter is formed that is both extremely dense and extremely hot, with an energy density of $\epsilon = 3 \text{ GeV per fm}^3$ (roughly 20 times that of normal matter) and an estimated temperature of $T = \sim 235 \text{ MeV}$ (roughly 3×10^{12}) (this is more



than 5 orders of magnitude hotter than the interior of the This new phase of matter grows explosively because of the steep pressure gradients present. After some fm/c (about 10^{-23} sec), the density drops by a factor of three, and the first hadronic elements of regular matter emerge from the highly excited state ("chemical freeze-out"). After a few times 10^{-23} sec, the system has cooled so much that thermally generated particles no longer have strong interactions and may fly freely to the detectors ("thermal freeze-out"), albeit still being very hot ($T \sim 175$ MeV). Time development of the resulting "fireball" in a plane perpendicular to the direction of the impact is seen on the right. When the system decouples from strong interactions at half the speed of light, it expands to a size twice that of the approaching projectile, in the direction where all the expansion is due to pressure gradients in the "fireball."

4.2 The phase diagram

[6] Heavy-ion collisions at the SPS produce temperatures and densities high enough to allow us to map our results onto the broader nuclear matter phase diagram. At high enough temperature and density, nuclear matter may exist in a deconfined state of quarks and gluons in addition to its typical hadronic form, just as water may exist in several phases (solid, liquid, gas). Studies at SIS and AGS got close to the region between the two phases (indicated by the green hatching zone), but the SPS tests were the first to obtain a good look at it. The expansion path of a fireball produced by Lead-on-Lead collisions at the SPS is also shown [7]"

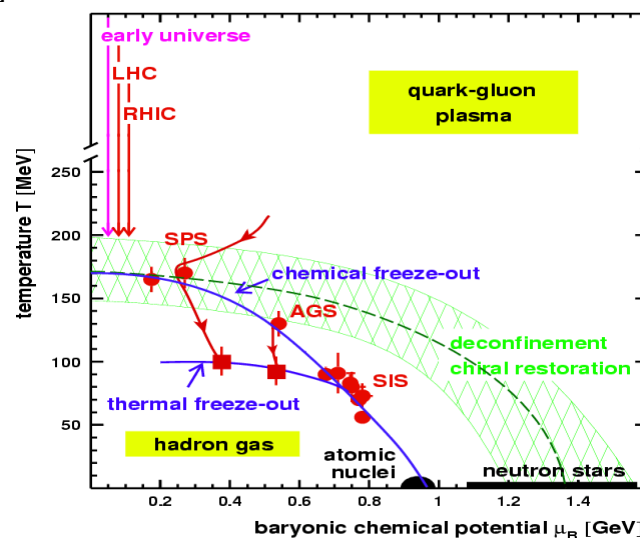


Figure 5 Baryonic chemical potential

[8] Characteristics of heavy ion collisions in general Extreme stretching occurs in nuclei at all length scales that matter in high-energy physics. Therefore, while attempting to make sense of experimental data, it is crucial to consider the geometry of the collision. In the center-of-



mass frame, both nuclei appear as thin disks, with their transverse diameters being dictated by Lorentz contraction along the longitudinal axis. One of the most important numbers is the impact parameter, which is the radial distance between the centers of the colliding nuclei. Each collision's "impact parameter" is very important. When the impact parameter is small, a head-on collision between the nuclei occurs, but when it is large, the collision occurs on the nuclei's periphery. Only the photons produced by the ions' powerful electromagnetic field allow for interaction between the two nuclei in the event of ultraperipheral collisions. For the second, $N_{part}[9]$ represents the total number of protons and neutrons in the nucleus. The remaining particles, called spectators, continue their trip mostly undamaged and are often detected in forward detectors like the Zero-Degree Calorimeter (ZDC) to assist locate the impact's epicenter. That's a lot of N_{colls} , or incoherent collisions between nucleons. [10]

5. FORMATION OF TWO-CENTER SHELL MODEL:

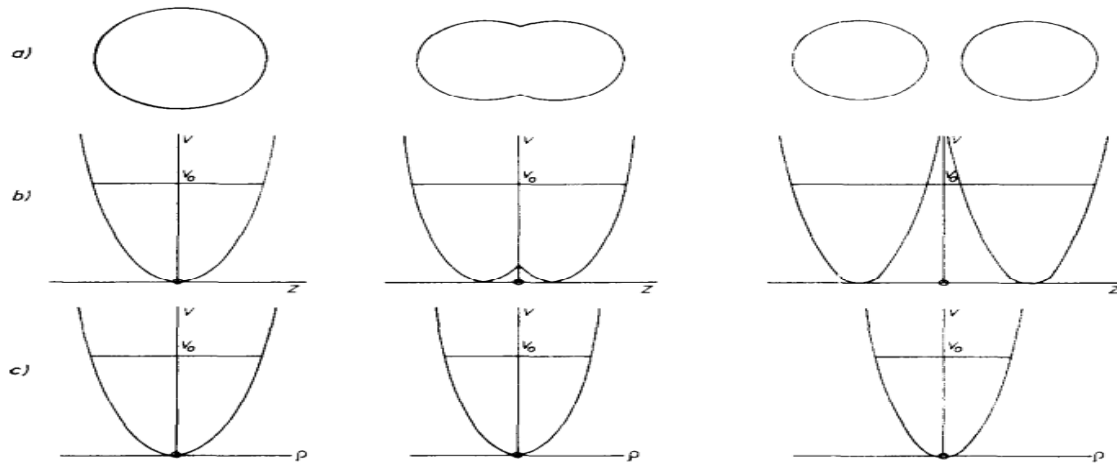


Figure 6 Two-center shell model:

“[11]Two-Center Shell Model (TC S M) was first established on the work of Holzer et al. Based on the double-center oscillator model, this inquiry inspired the creation of an asymptotically two-center shell model that incorporates spinorbit and angular momentum dependent components in a natural manner.

Its refined potential is expressed in cyclic notation as

$$E(\tau, c) = \frac{1}{2} K [\pi_{\tau}^2 \tau^2 + \pi^2 c'^2 F_0 (1 + zc' + tc'^2)] \quad (1)$$

where K is the nucleon mass ($\frac{K}{12} = 0.024106 \text{ MeV} \cdot \text{fm}^{-2}$). The Hamiltonian of the TC S M has the form

$$L = -\frac{1}{2} \Delta^2 / K + E(\tau, c) + E_{/o}(Y, X, \theta) + E_{h^2}(h) \quad (2)$$

The spin-orbit potential $V_{/o}$ is of Thomas-type



$$E_{/o} = -\frac{2Hp}{K\pi_{\approx}} [\Delta E(\rho, c) \times X] \cdot 8 \quad (3)$$

The E_{h^2} - potential of the Nilsson model cannot be adapted in an analogous form, because there exists no set of the parameters $\{p, \delta\}$ that reproduce the observed level sequence. Therefore, we keep the h^2 -term in the usual manner [3, 12]

$$E_{h^2} = -H\pi_{\approx} p\delta \left[h^2 - \frac{1}{2} n(n+3) \mu_{if} \right] \quad (4)$$

where π_{\approx} is the asymptotic frequency of the colliding nuclei. Further, means that we are considering only the contribution of the diagonal matrix elements. As usual for the phenomenological shell model, we identify the equipotential surface

$$E_{\emptyset} = \frac{1}{2} K\pi_{\approx}^2 C_0^2 \quad (5)$$

as a nuclear surface. C_0 is the equivalent uniform radius that can be calculated from $r.m.s.$ radius $\langle C^2 \rangle^{1/2}$ by $C_s = \left(\frac{5}{3} \langle C^2 \rangle^{1/2}\right)$. We only notice that the spectra show the desirable asymptotic behaviour in both, the sudden and the adiabatic case

[13] Here we need the energy levels for the calculation of the shell corrections. Therefore, we take only as many basis states as needed for their convergence to 10 keV accuracy. We found that we need, e.g. 150 basis states for $r^{12}R-^{12}R$ the and 600 basis states for $^{238}J-^{238}J$ -system. While for the basis one only has to calculate the quantum numbers as function of the deformation, the definition of some interpolation prescription for the strength coefficients Q , and δ of the E_{h^0} and E_{h^2} terms as a function of the deformation parameters is needed. The initial values a_g and δ_a ; for the in-dependent nuclei and the final values a_F and δ_F of the compound nucleus are well known. In the sudden case we want to conserve the individual properties of the colliding nuclei, so we set $a(\beta_g) = a_F = a_g$ and $\delta(\beta_g) = \delta_F = \beta_g$ without any interpolation. The adiabatic process is characterized by the volume conservation. The compound nucleus is going to have a_F and δ_F values that are different from those of the two individual nuclei [14]. In the interpolation prescription we use, a , and δ depend only indirectly on the deformation parameters. We define namely the "intermediate mass number" $P(\beta_g)$ as follows:

$$P(\beta_g) = \frac{2P_{\approx}}{\alpha(\beta_g)} \quad (6)$$

with $\alpha(\beta_g)$

$$= \begin{cases} \left\{ 1 + l^2 \exp \left\{ -\left(P_{\approx} / 100c \right) \right\} \right\} & \text{for } l \leq 1 \\ 2 & \text{for } l > 1 \end{cases}$$

and put $a\beta_g = a[P(\beta_g)]$, $\delta(\beta_g) = \delta[P(\beta_g)]$ according to Figure 7. Due to this interpolation the nuclei have their touching point ($l=1$) at increasing relative distances ($2c_0$) with increasing nucleon number P_{\approx} . Furthermore, in the overlap region the nuclear shapes without or with only a small neck-in are energetically preferred, as expected.

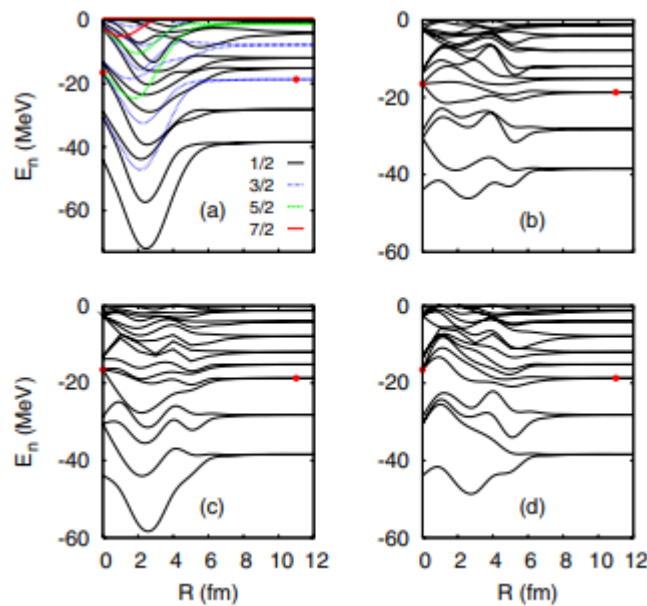


Figure 7 Nuclei interpolation

ii) For nonaxial symmetric configurations, the neutron levels show a minimum at separations between 4–6 fm, which may result in a “molecular pocket” in the collective potential energy surface. This depends weakly on the mutual alignment. (iii) Many avoided crossings appear between 2–6 fm, in which the SP wave function abruptly changes its nodal structure. It may lead to strong peaks in the radial collective mass parameter, which can hinder the fusion of the nuclei. The critical radius for fusion (where the shell structure of ^{24}Mg starts to build up) is quite small for nonaxial symmetric configurations (≈ 2 fm), which also favors the formation of a nuclear molecule (the weakly overlapping nuclei remain longer around 4–6 fm). The preservation of the identity of the nuclei along with their being trapped around the contact distance are crucial aspects for the formation of a nuclear molecule. These favorable features are shown by nonaxial symmetric configurations of $^{12}\text{C} \text{ } ^{12}\text{C}$. Since their shell structures are quite similar, the ^{12}C orientation is clearly an essential variable in the reaction processes. This degree of freedom activates dynamical modes (butterfly, antibutterfly, belly dancer, etc.) at contact, making the nuclei “dance” there for quite some time. It should result in narrow resonances in the reaction cross sections, as shown by measurements [15]. The molecular SP spectra are useful to microscopically obtain collective potentials and mass surfaces for a molecular reaction dynamical calculation. It is worth mentioning that other studies have also argued the importance of the nonaxial symmetric configurations for effects of molecular resonances on reaction processes for $^{12}\text{C} \text{ } ^{12}\text{C}$ [16].

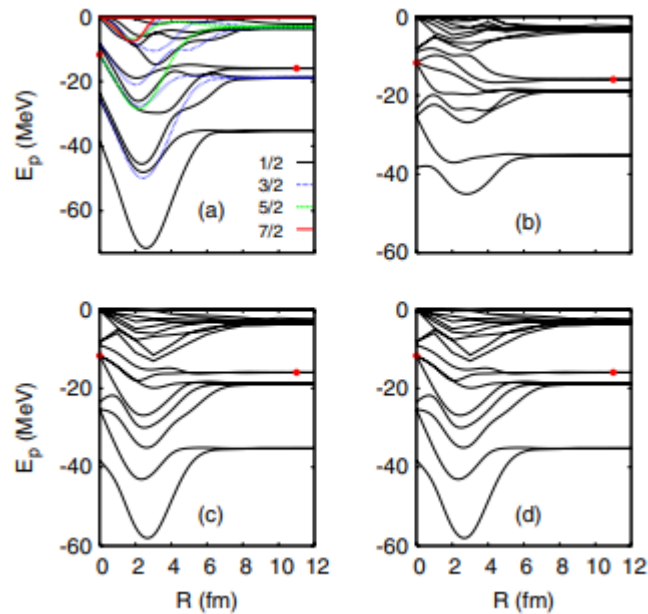


Figure 8 R vs. E_p

6. CONCLUSION

As this short introduction to the theoretical characteristics of heavy ion collisions with a single center shell model concludes, it is important to keep in mind the challenge of characterizing a massive, time-dependent, non-equilibrated system in terms of a (quite intricate) underlying microscopic theory (QCD). Though we haven't spent much time on it, it's important to note that many observables in heavy ion collisions depend on a number of mundane aspects of low energy nuclear physics, such as the shape and size of the nuclei, as well as the distribution of the nucleons within a nucleus and the fluctuations. Despite the fact that these are not the primary goals of the heavy-ion collision program, they are crucial when attempting to infer a QCD attribute from experimental data. Numerous characteristics of the quarkgluon plasma have been found via a combination of experimental and theoretical efforts: Its equation of state is consistent with lattice QCD expectations and with the deconfinement of the color degrees of freedom, the yield of "light" partons, including charm quarks, is significantly suppressed compared to rescaled proton-proton collisions, and the suppression of bottom quarks is even more pronounced. At the highest energies, the production of charm quarks is abundant enough to lead to the formation of J/ψ bound states by recombination of uncorrelated quarks and antiquarks, which has allowed us to determine that a large amount of energy is radiated by soft emissions at large angle. There have been many breakthroughs, but it is also clear that, despite these successes, it is still very challenging to extract the underlying QCD properties from the result of heavy ion collisions, as in several cases the comparisons



with QCD have remained rather qualitative despite the detail of the experimental measurements. Furthermore complicating matters is the fact that some of these investigations compare the results of proton-proton or proton-nucleus collisions with those of rescaled proton-nucleus or proton-proton collisions. High energy proton-nucleus and proton-proton collisions, however, have turned out to exhibit certain traits similar to those reported in nucleus-nucleus collisions, putting some concerns on their utility as "references" to compare with in order to identify phenomena exclusive to the quark-gluon plasma. It may be necessary to adjust to life without this frame of reference for certain observables if it turns out that flow occurs even in proton-proton collisions. Our key finding is the demonstration of a novel method for solving the two-center issue using distorted realistic potentials of any orientation. Cluster physics aside, this should be particularly helpful for describing, within the molecular picture, low energy nuclear reaction processes involving deformed nuclei, such as (i) the formation of heavy and superheavy elements, (ii) the effects of breakup of weakly bound nuclei on fusion, and (iii) fusion reactions of great astrophysical interest. Molecular spin-parity (SP) spectra reveal that nonaxial symmetric configurations are required for the production of a nuclear molecule in the reaction $^{12}\text{C} + ^{12}\text{C}$. The astrophysical significance of molecular resonance structures is now the subject of reaction dynamical simulations.

References

- [1] J. Maruhn and W. Greiner, "The asymmetric two center shell model," *Zeitschrift für Physik*, vol. 251, pp. 431-457, 1972.
- [2] F. Gelis, "Some aspects of the theory of heavy ion collisions," *Reports on Progress in Physics*, vol. 84, p. 056301, 2021.
- [3] M. He, B. Wu, and R. Rapp, "Collectivity of J/ψ Mesons in Heavy-Ion Collisions," *Physical Review Letters*, vol. 128, p. 162301, 2022.
- [4] Y.-L. Du, D. Pablos, and K. Tywoniuk, "Deep learning jet modifications in heavy-ion collisions," *Journal of High Energy Physics*, vol. 2021, pp. 1-50, 2021.
- [5] S. Choudhury, X. Dong, J. Drachenberg, J. Dunlop, S. Esumi, Y. Feng, et al., "Investigation of experimental observables in search of the chiral magnetic effect in heavy-ion collisions in the STAR experiment," *Chinese Physics C*, vol. 46, p. 014101, 2022.
- [6] Y. Sun, V. Greco, and X.-N. Wang, "Modification of Z^0 leptonic invariant mass in ultrarelativistic heavy ion collisions as a measure of the electromagnetic field," *Physics Letters B*, vol. 827, p. 136962, 2022.
- [7] R. K. Gupta, M. K. Sharma, N. Antonenko, and W. Scheid, "On the absence of an-nucleus structure in a two-centre shell model," *Journal of Physics G: Nuclear and Particle Physics*, vol. 25, p. L47, 1999.



Received: 16-01-2024

Revised: 12-02-2024

Accepted: 07-03-2024

- [8] D. Ivanishchev, D. Kotov, M. Malaev, V. Riabov, and Y. Riabov, "STUDY OF Φ (1020) AND $K^*(892)$ MESON PRODUCTION IN HEAVY-ION COLLISION AT NICA-MPD," in PARTICLE PHYSICS at the Year of 150th Anniversary of the Mendeleev's Periodic Table of Chemical Elements: Proceedings of the Nineteenth Lomonosov Conference on Elementary Particle Physics, 2021, pp. 345-349.
- [9] J. Steinheimer, A. Motornenko, A. Sorensen, Y. Nara, V. Koch, and M. Bleicher, "The high-density equation of state in heavy-ion collisions: constraints from proton flow," The European Physical Journal C, vol. 82, pp. 1-12, 2022.
- [10] Y. Nara and A. Ohnishi, "Mean-field update in the JAM microscopic transport model: Mean-field effects on collective flow in high-energy heavy-ion collisions at $\sqrt{s_{NN}} = 2-20$ GeV energies," Physical Review C, vol. 105, p. 014911, 2022.
- [11] S. Singh and R. Gupta, "A few nucleon to large mass transfer in heavy-ion reactions using dynamical theory based on two centre shell model," in DAE symposium on nuclear physics: invited talks/seminars. Vol. 35A (1992), 1992.
- [12] Z.-t. Liang, "Spin Effects In Heavy Ion Collisions at High Energies," arXiv preprint arXiv:2203.09786, 2022.
- [13] M. H. E. Abu-Sei'leek, "Excitation of the delta-resonance in compressed super heavy neutron-rich doubly magic $U_{126}^{106}Bi_{184}^{184}$ nucleus," Nuclear Physics A, vol. 1027, p. 122522, 2022.
- [14] T. Vockerodt, "Quantum dynamics of heavy-ion collisions at Coulomb energies using the time-dependent coupled-channel wave-packet method," 2021.
- [15] E. Shuryak, "The heavy ions are "preheated" prior to high energy collisions," arXiv preprint arXiv:2201.11064, 2022.
- [16] B. Zakharov, "Jet quenching from heavy to light ion collisions," Journal of High Energy Physics, vol. 2021, pp. 1-30, 2021.